Supplement of

Summertime aerosol volatility measurements in Beijing, China

Weiqi Xu[1,2], Conghui Xie[1,2], Eleni Karnezi[3,a], Qi Zhang[4], Junfeng Wang[5], Spyros N. Pandis[3], Xinlei Ge[5], Qingqing Wang[1], Jian Zhao[1,2], Wei Du[1,2,b], Yanmei Qiu[1,2], Wei Zhou[1,2], Yao He[1,2], Jingwei Zhang[1,2], Junling An[1,2], Ying Li[1], Jie Li[1], Pingqing Fu[2,6], Zifa Wang[1,2], Douglas R. Worsnop[7], and Yele Sun[1,2,8*]

[1]State Key Laboratory of Atmospheric Boundary Layer Physics and Atmospheric Chemistry, Institute of Atmospheric Physics, Chinese Academy of Sciences, Beijing 100029, China
[2]University of Chinese Academy of Sciences, Beijing 100049, China
[3]Department of Chemical Engineering, Carnegie Mellon University, Pittsburgh, PA, USA
[4]Department of Environmental Toxicology, University of California, 1 Shields Ave., Davis, California 95616, United States
[5]School of Environmental Science and Engineering, Nanjing University of Information Science & Technology, Nanjing 210044, China
[6]Institute of Surface-Earth System Science, Tianjin University, Tianjin 300072, China
[7]Aerodyne Research Inc., Billerica, Massachusetts 01821, USA
[8]Center for Excellence in Regional Atmospheric Environment, Institute of Urban Environment, Chinese Academy of Sciences, Xiamen 361021, China
[a]now at: Earth Sciences Department, Barcelona Supercomputing Center, BSC-CNS, Barcelona 08034, Spain
[b]now at: Department of Physics, University of Helsinki, P.O. Box 64, 00014 Finland

Correspondence: Yele Sun (sunyele@mail.iap.ac.cn)

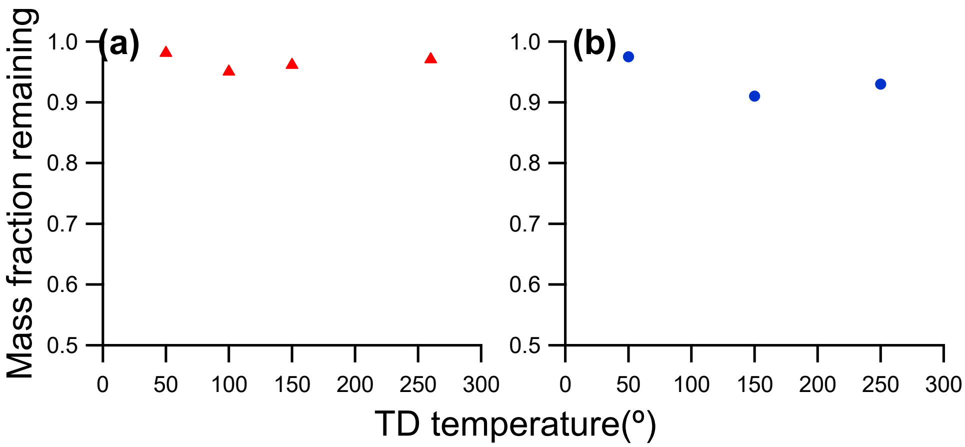

Figure S1. Particle mass loss within the thermal denuder in summer of (a) 2017 and (b) 2018.

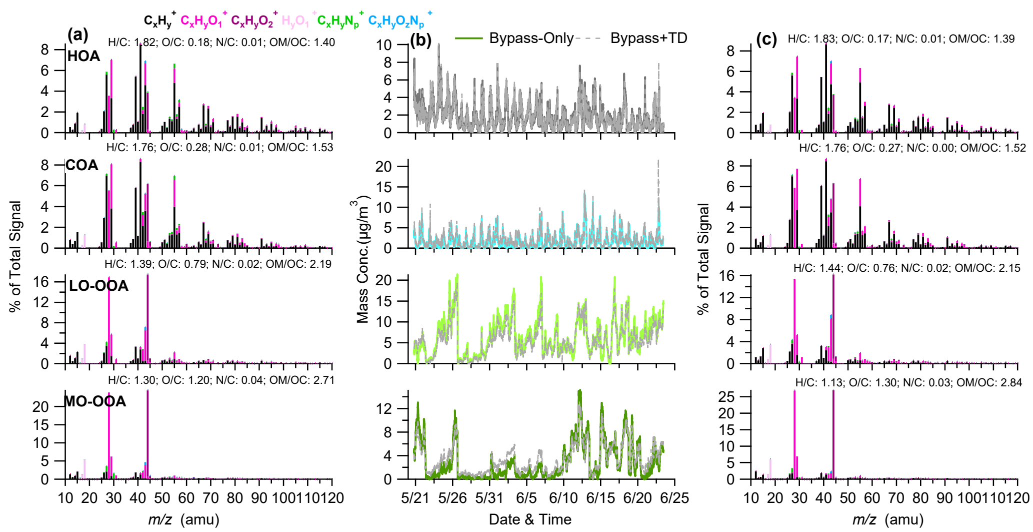

Figure S2. Mass spectra of OA factor resolved by (a) $MS_{ambient}$ and (c) $MS_{ambient+TD}$ using ME-2 analysis. (b) shows a comparison of time series of OA factor resolved from $MS_{ambient}$ and $MS_{ambient+TD}$ in summer 2018.

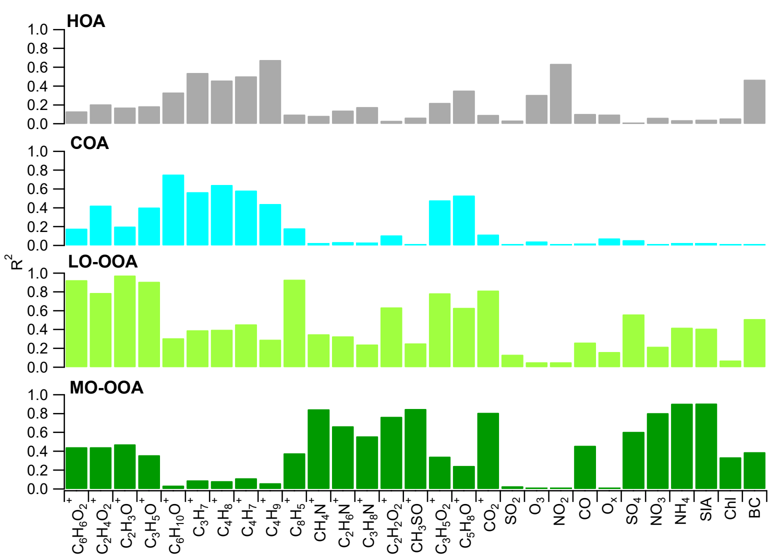

Figure S3. Correlation between OA factors and tracers in summer 2018.

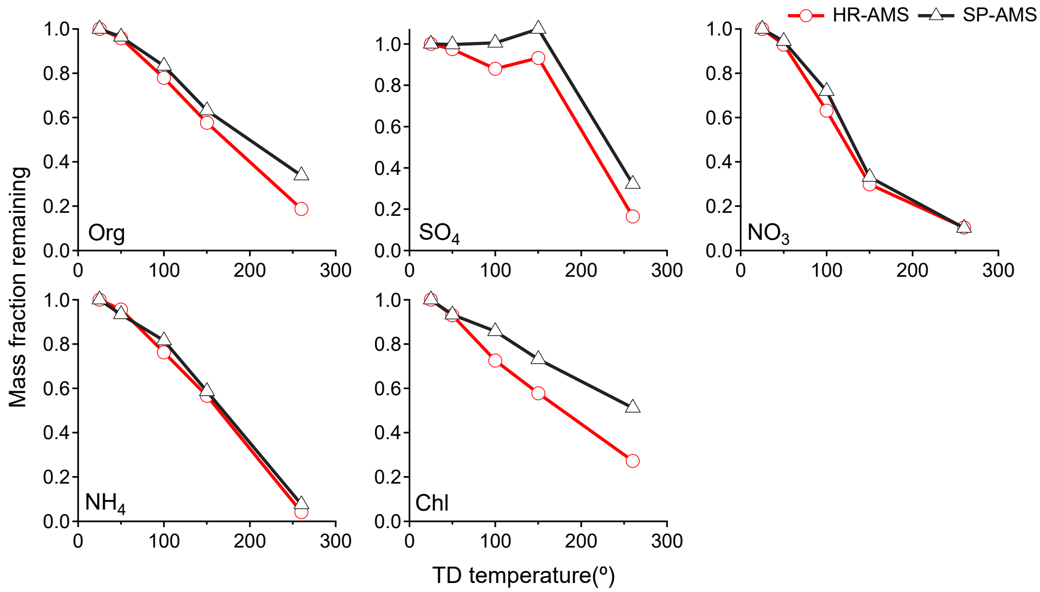

Figure S4. Thermograms of aerosol species measured by TD-HR-AMS and TD-SP-AMS in 2017.

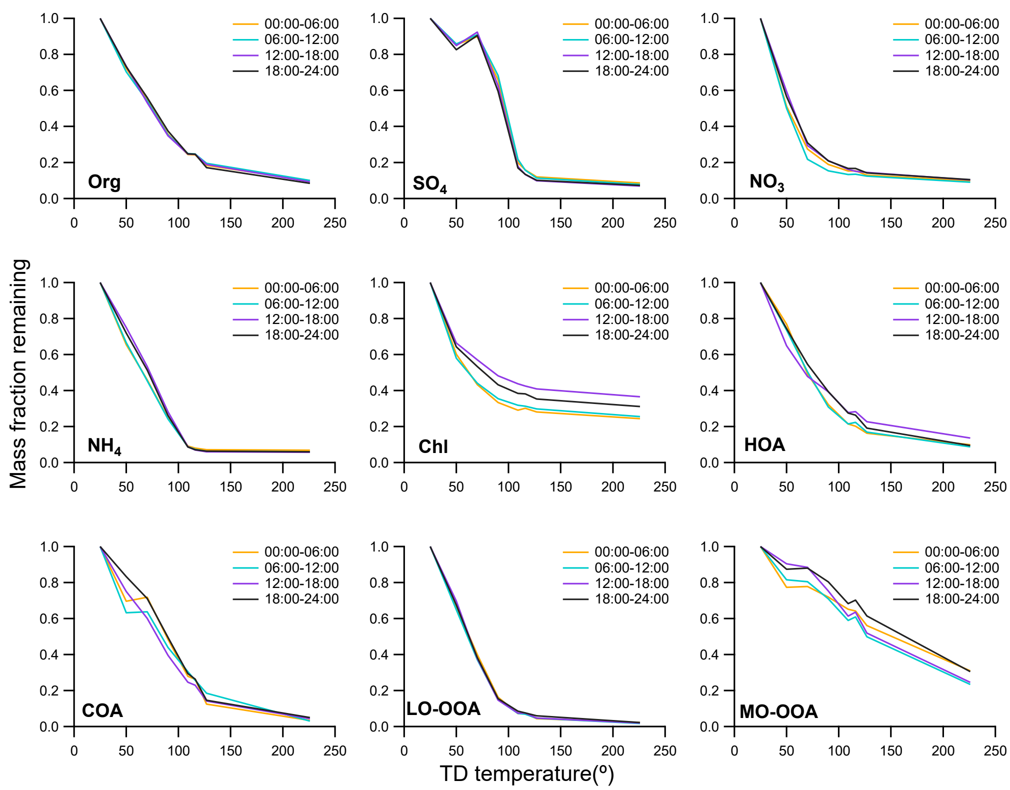

Figure S5. Thermograms of aerosol species and OA factors during four different time periods in 2018.

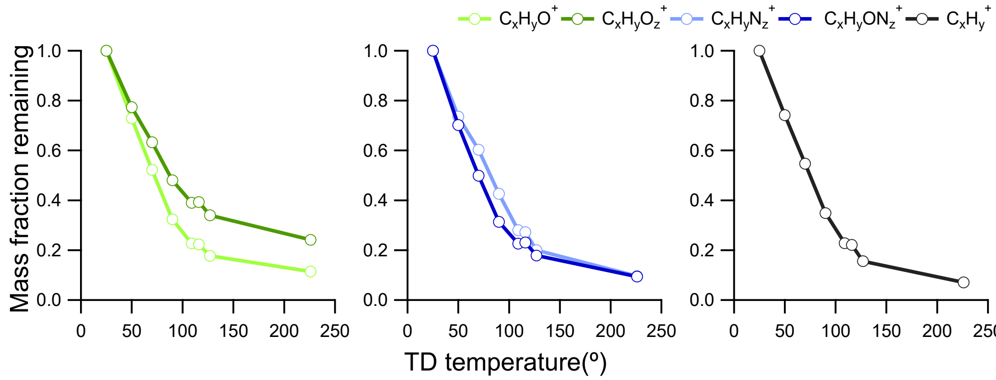

Figure S6. Thermograms of four different ion families in summer 2018.

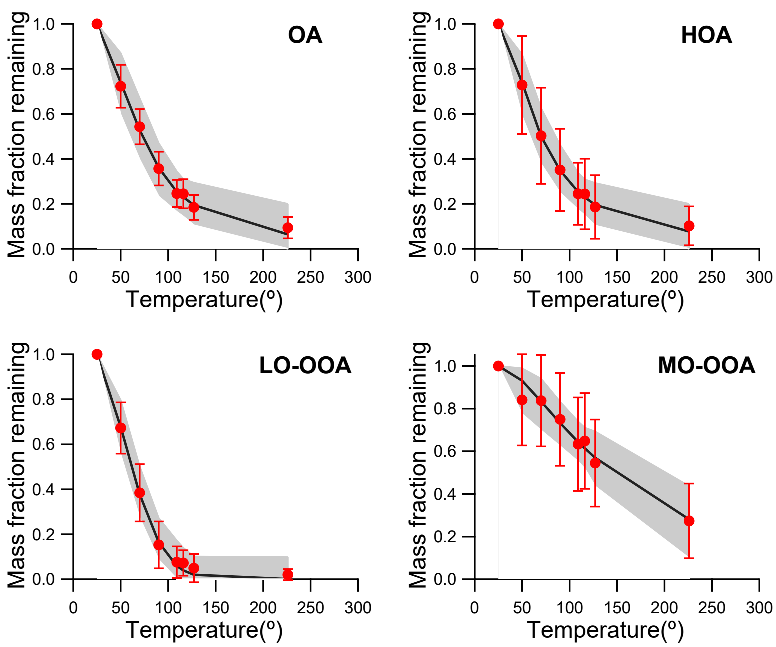

Figure S7. Thermograms of OA and OA factors measured by TD-HR-AMS in 2018. The solid circles represent the measurements and the error bars are one standard deviation. The black lines refer to the best-predicted MFR using the algorithm of Karnezi et al. (2014)

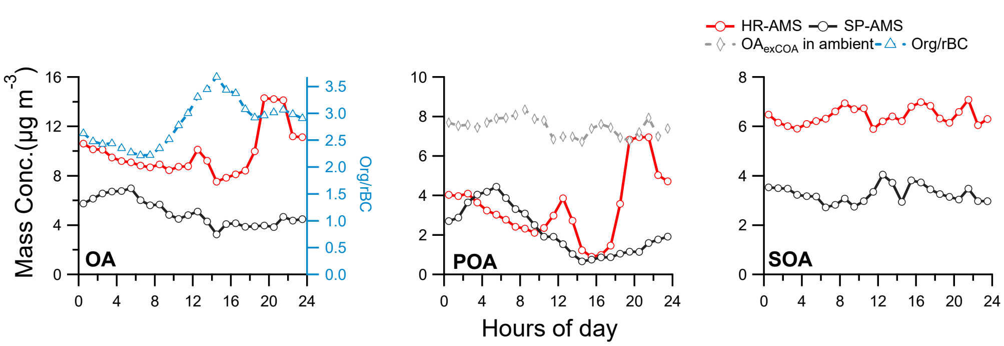

Figure S8. Average diurnal cycles of Org/rBC ratio, and mass concentrations of ambient and BC-containing OA, POA and SOA.

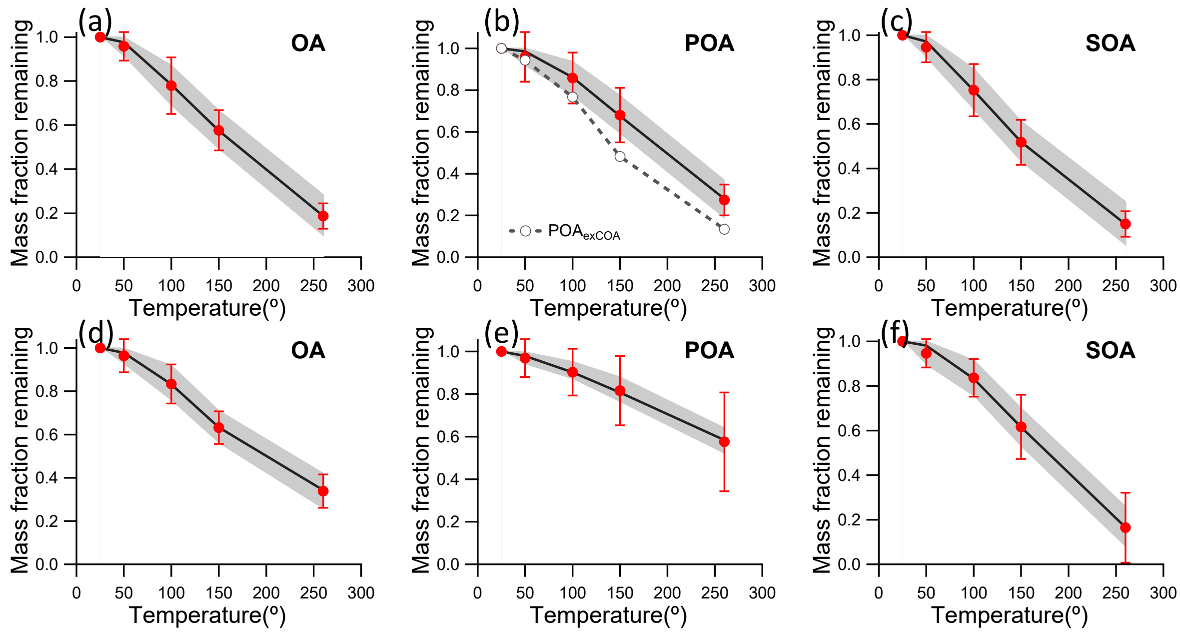

Figure S9. Thermograms of OA, POA and SOA factors measured by (a,b,c) TD-HR-AMS and (d,e,f) TD-SP-AMS in 2017. The solid circles represent the measurements, and the error bars are one standard deviation. The black lines refer to the best-predicted MFR using the algorithm of Karnezi et al. (2014)

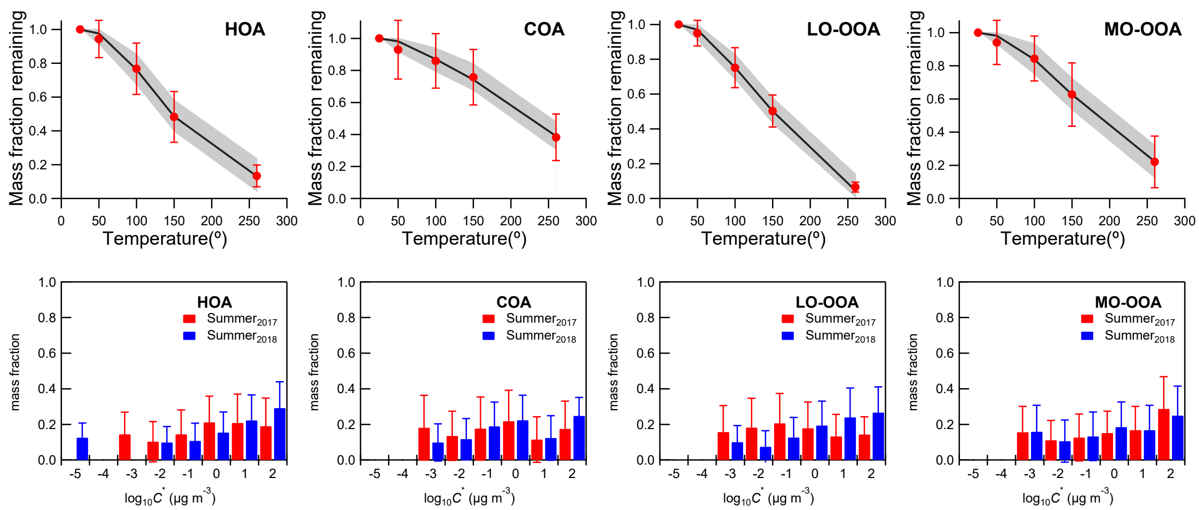

Figure S10. Thermograms and predicted volatility distributions of four OA factors measured by TD-HR-AMS in 2017. The solid circles represent the measurements and the error bars are one standard deviation. The black lines refer to the best-predicted MFR using the algorithm of Karnezi et al. (2014). The error bars in bottom panels are the uncertainties derived using the approach of Karnezi et al. (2014). Predicted volatility distributions of four OA factors in 2018 are also shown for comparisons.

Table S1. Average ambient concentrations, threshold concentrations for PM species and OA factors and corresponding fraction of the data above the threshold.

	Average mass concentration ($\mu g\ m^{-3}$)	Threshold concentration ($\mu g\ m^{-3}$)	% of measurements above threshold
HR-AMS$_{2018}$			
Org	12.7	1.5	99.6%
SO_4	6.5	0.4	99.7%
NO_3	7.4	0.06	99.6%
NH_4	4.3	0.16	99.6%
Chl	0.18	0.02	98.6%
HOA	1.7	0.05	97.6%
COA	2.0	0.04	97.6%
LO-OOA	5.8	0.4	97.2%
MO-OOA	3.4	0.5	98.5%
HR-AMS$_{2017}$			
Org	9.8	2.98	97.6%
POA	3.4	0.48	99.5%
HOA	1.0	0.19	98.9%
COA	2.4	0.16	96.4%
SOA	6.4	1.31	98.2%
LO-OOA	3.8	1.01	97.6%
MO-OOA	2.6	0.12	98.6%
SP-AMS$_{2017}$			
Org	5.5	1.3	98.6%
POA	2.2	0.41	96.7%
SOA	3.3	0.81	97.7%

Table S2. Best fit OA volatility parameter values in previous field studies.

Species	Volatility distribution											ΔH	a_m
	10^{-8}	10^{-7}	10^{-6}	10^{-5}	10^{-4}	10^{-3}	10^{-2}	10^{-1}	10^{0}	10^{1}	10^{2}		
OA[a]						0.2	0.2	0.3	0.3			80	1
OA[a]							0.2	0.2	0.3	0.3		80	0.05
HOA[b]					0.13	0.14	0.08	0.02	0.06	0.57		100	1
COA[b]				0.13	0.15	0.07	0.2	0.08	0.37			100	1
MOA[b]					0.03	0.03	0.05	0.28	0.42	0.19		100	1
SV-OOA[b]					0.06	0.14	0.15	0.13	0.18	0.34		100	1
LV-OOA[b]		0.2	0.24	0.28	0.25	0.03						100	1
HOA[c]					0.11	0.09	0.07	0.12	0.11	0.5		100	1
COA[c]			0.12	0.11	0.14	0.42	0.11	0.1				100	1
BBOA[c]					0.2	0.09	0.08	0.13	0.09	0.41		100	1
OOA[c]					0.3	0.09	0.07	0.09	0.1	0.35		100	1
OA[d]	0.3					0.08	0.12	0.12	0.12	0.26		100	1
OOA[d]	0.41					0.11	0.09	0.08	0.11	0.2		100	1
HOA[d]	0.3					0.07	0.14	0.21	0.17	0.11		100	1
BBOA[d]	0.1					0.1	0.15	0.15	0.14	0.36		100	1
COA[d]	0.1					0.52	0.08	0.05	0.07	0.18		100	1
OA[e]					0.14	0.05	0.06	0.15	0.29	0.31		100	0.5
OA[f]					0.14	0.06	0.08	0.12	0.28	0.32		100	0.5
MO-OOA[g]								0.44	0.14	0.42		89	1
LO-OOA[g]								0.27	0.19	0.54		58	1
isoprene-OA[g]								0.41	0.16	0.43		63	1
BBOA[g]								0.47	0.29	0.24		55	1
OA[g]								0.54	0.19	0.27		86	1
OA[h]			0.06	0.06	0.06	0.07	0.07	0.08	0.10	0.16	0.34	100	1
OA[h]					0.27	0.11	0.11	0.12	0.15	0.24		100	1
OA[h]			0.04	0.04	0.04	0.04	0.05	0.06	0.1	0.2	0.43	100	0.1
OA[h]					0.21	0.07	0.09	0.10	0.18	0.35		100	0.1

[a] Sampling site is Finokalia, and the sampling time is May, 2008. (Lee et al., 2010). This estimation use the transfer model of Riipinen et al. (2010) with least-squares minimization. Assumed a priori values for the effective vaporization enthalpy with 80 KJ mol^{-1} and the mass accommodation coefficient with 1/0.05.

[b and C] Sampling site is Paris, and the sampling time is July, 2009 and January/February 2010, respectively(Paciga et al., 2016). This estimation use the transfer model of Riipinen et al. (2010), and the uncertainties are calculated by Karnezi et al. (2014). Assumed a priori values for the effective vaporization enthalpy with 100 KJ mol^{-1} and the mass accommodation coefficient with 1.

[d] Sampling site is Athens, and the sampling time is January/February 2013 (Louvaris et al., 2017). This estimation use the transfer model of Riipinen et al. (2010), and the uncertainties are calculated by Karnezi et al. (2014). Assumed a priori values for the effective vaporization enthalpy with 100 KJ mol^{-1} and the mass accommodation coefficient with 1.

[e and f] Sampling site is Centreville and Raleigh, and the sampling time is June/July and Nov./Oct. 2013, respectively (Saha et al., 2017). This estimation use the volatility parameter extraction framework(Saha et al., 2015) to extract a set of volatility parameter (C^*, Hvap, γe) values via inversion of dual-TD data using an evaporation kinetics model.

[g] Sampling site is Centreville, and the sampling time is June/July 2013 (Kostenidou et al., 2018). This estimation use the transfer model of Riipinen et al. (2010), and the uncertainties are calculated by Karnezi et al. (2014). The enthalpy of vaporization was also estimated, while the accommodation coefficient was assumed to be equal to unity.

[h] Sampling site is Mexico City, and the sampling time is March/April 2006(Cappa and Jimenez, 2010)

References

Cappa, C. D., and Jimenez, J. L.: Quantitative estimates of the volatility of ambient organic aerosol, Atmos. Chem. Phys., 10, 5409-5424, 10.5194/acp-10-5409-2010, 2010.

Karnezi, E., Riipinen, I., and Pandis, S. N.: Measuring the atmospheric organic aerosol volatility distribution: a theoretical analysis, Atmospheric Measurement Techniques, 7, 2953-2965, 10.5194/amt-7-2953-2014, 2014.

Kostenidou, E., Karnezi, E., Hite Jr, J. R., Bougiatioti, A., Cerully, K., Xu, L., Ng, N. L., Nenes, A., and Pandis, S. N.: Organic aerosol in the summertime southeastern United States: components and their link to volatility distribution, oxidation state and hygroscopicity, Atmos. Chem. Phys., 18, 5799-5819, 10.5194/acp-18-5799-2018, 2018.

Lee, B. H., Kostenidou, E., Hildebrandt, L., Riipinen, I., Engelhart, G. J., Mohr, C., DeCarlo, P. F., Mihalopoulos, N., Prevot, A. S. H., Baltensperger, U., and Pandis, S. N.: Measurement of the ambient organic aerosol volatility distribution: application during the Finokalia Aerosol Measurement Experiment (FAME-2008), Atmos. Chem. Phys., 10, 12149-12160, 10.5194/acp-10-12149-2010, 2010.

Louvaris, E. E., Florou, K., Karnezi, E., Papanastasiou, D. K., Gkatzelis, G. I., and Pandis, S. N.: Volatility of source apportioned wintertime organic aerosol in the city of Athens, Atmos. Environ., 158, 138-147, 10.1016/j.atmosenv.2017.03.042, 2017.

Paciga, A., Karnezi, E., Kostenidou, E., Hildebrandt, L., Psichoudaki, M., Engelhart, G. J., Lee, B.-H., Crippa, M., Prevot, A. S. H., Baltensperger, U., and Pandis, S. N.: Volatility of organic aerosol and its components in the megacity of Paris, Atmos. Chem. Phys., 16, 2013-2023, 10.5194/acp-16-2013-2016, 2016.

Riipinen, I., Pierce, J. R., Donahue, N. M., and Pandis, S. N.: Equilibration time scales of organic aerosol inside thermodenuders: Evaporation kinetics versus thermodynamics, Atmos. Environ., 44, 597-607, 10.1016/j.atmosenv.2009.11.022, 2010.

Saha, P. K., Khlystov, A., and Grieshop, A. P.: Determining Aerosol Volatility Parameters Using a “Dual Thermodenuder” System: Application to Laboratory-Generated Organic Aerosols, Aerosol Sci. Tech., 49, 620-632, 10.1080/02786826.2015.1056769, 2015.

Saha, P. K., Khlystov, A., Yahya, K., Zhang, Y., Xu, L., Ng, N. L., and Grieshop, A. P.: Quantifying the volatility of organic aerosol in the southeastern US, Atmos. Chem. Phys., 17, 501-520, 10.5194/acp-17-501-2017, 2017.